NUMERICAL AND EXPERIMENTAL STUDY ON SHEAR BEHAVIOR OF RC DEEP BEAMS AND WALL-TYPE PIERS

Mohammad Reza SALAMY[1], Hiroshi Kobayashi[2] and Shigeki Unjoh[3]

Abstract

A study on RC deep beams and wall-type piers behavior is presented in this paper by means of finite element analysis along with experimental evaluation. Although the application of those two structures is different but their behavior is similar if shear dominates the failure mode. In both members, shear resisting mechanism is improved by means of arch action which increase shear capacity of the member. Shear span to depth ration a/d has an important role in shear resisting mechanism where in member's shear capacity can be improved substantially. In this study investigated members have a range of a/d=0.5, 1.0 and 1.5.

Introduction

The primary objective of this study is to investigate behavior of underground structures subjected to up filled materials weight as well as seismic excitation. It is found, however, that in such structures, members are likely to behave similar to RC deep beams since span to depth ratio will be small. During an earthquake it is evident that a shear force is produced in structure's circumference leads to shear deformation of entire structure associated with earth pressure in lateral and vertical direction (Fig.1). Such loading results large section in resisting members which in span to depth ratio will be likely similar to deep beams definition. This is the main objective of the study to investigate behavior of those members experimentally and analytically for engineering practical purpose and improvement of current design codes dealing with design of underground structures. Three sets of specimens comprise of nineteen RC beams are investigated in this study. The beams have shear span to depth ratio between 0.5 and 1.5 and effective depth size from 400 mm to 1400 mm. The longitudinal tensile reinforcement ratio is kept almost constant in about 2% for all specimens while lateral reinforcement (stirrups) ratio varies by 0.0%, 0.4% and 0.8% in shear span. A codified study on foregoing experiment is presented elsewhere [Salamy *at al*, 2005].

In order to perform nonlinear finite element analysis on RC members, proper models for concrete material and cracked concrete should be carefully selected. So far a

---

[1] Dr. Eng., Senior research engineer, Earthquake Engineering Research Team, Public Works Research Institute, Japan
[2] Information System Planning Group, Hanshin Expressway Company Ltd, Osaka, Japan
[3] Dr. Eng., Leader of Earthquake Engineering Research Team

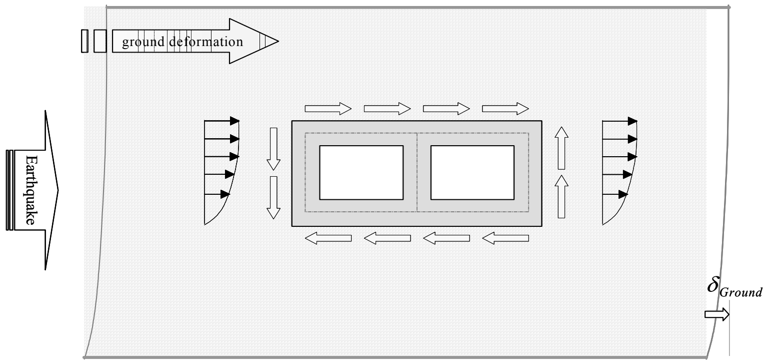

FIG.1. UNDERGROUND STRUCTURES UNDER SEISMIC LOAD

wide range of material models have been proposed by researchers during recent decades. The obstacle in any analysis is how to select the model fits best to the given problem in among large number of available models. It is noted, however, there is no consensus on what model results the best. In other words each model suits perhaps only particular problem. In original study, smeared crack model is examined by means of the fixed crack and the rotating crack approach. It is found that the rotating crack model results closer to experiment response than that of the fixed crack model. The latter approach suffers discrepancy in shear retention factor definition which is left to be analyzer choice. The problem manifests itself when shear failure dominates mode of failure which in significant sensitivity to the choice of shear retention factor is resulted. Although sensitivity of the results to shear retention factor is believed to be negligible in flexural mode of failure [Kwak, H., and Flippou F.C., 1990] but it is evident that variation of this factor has significant effect on results. In this paper only the results of analyses by means of the rotating crack model are presented. Fracture mechanics concept is utilized in order to eliminate sensitivity of response to mesh discretization which is usually observed in simulation of highly nonlinear material such as concrete and other type of brittle materials. The results of this study are also used to investigate behavior of RC wall-type piers under cyclic loads as well which are supposed to behave like deep beams if bending capacity cannot be achieved. In such case shear failure is the most probable failure mode the structure may experience. Two specimens of wall-type piers have been tested and analyzed here by means of the finite element method presented in the first part and will be presented at the end of this paper.

Specimens Details

Nineteen RC beams tested in this study with geometric characteristic and material properties given in Fig.2, Table 1 and Table 2. In Table 1, p_w, p_s, f_y, A_{st} and A_{sc} are shear span, stirrups ratio, longitudinal tensile reinforcement ratio and their yield stress, cross section area of tensile and compressive rebar respectively. All specimens, with or without stirrups in shear span, have a minimum lateral reinforcement in mid-span and out of span. Despite absence of shear stress in this part, which in the first look implies un-necessities of

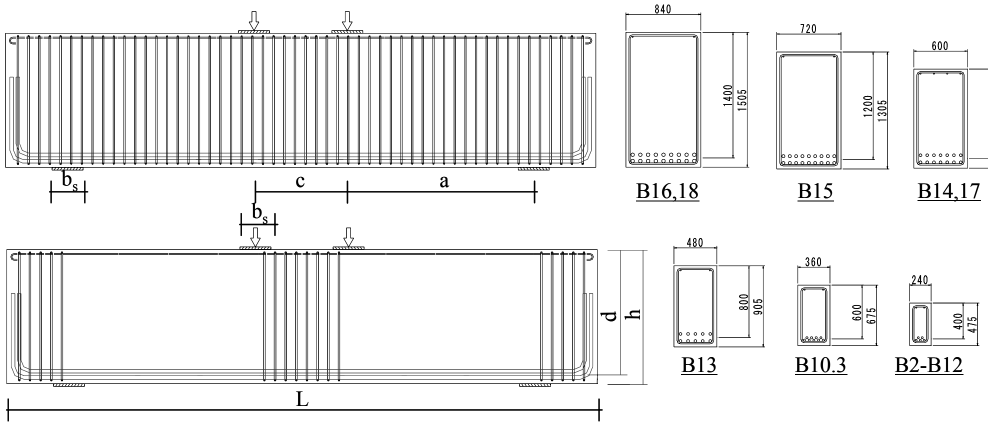

FIG.2. DETAIL OF SPECIMENS WITH AND WITHOUT STIRRUPS (UNIT: MM)

shear reinforcement, they may delay or in some case prevent the propagation of diagonal crack to compression zone. Since all specimens tested here have a minimum amount of stirrups at mid-span, it is however not possible to investigate lateral reinforcement effect located in that region.

In Table 2, b is specimen width, a/d and f'_c are shear span to depth ratio and compressive stress respectively. Maximum load capacity and related deflection as well as shear crack initiation load and maximum deflection are noted as P_{max}, P_{cr}^{sh}, δ_{peak} and $\delta_{\max}$ respectively. Other geometrical parameters of Table.2 are schematically determined in Fig.2. All specimens are subjected to four points monotonic static load condition.

TABLE 1. STEEL PROPERTIES OF SPECIMENS

Beam	ρ_w %	ρ_{st} %	f_y MPa	Ast Asc	Stirrups
B2	0.0	2.02	376	5D22 2D10	
B3	0.4				D6@65
B4	0.8				D10@75
B6	0.0				
B7	0.4				D6@65
B8	0.8				D10@75
B10-1	0.0				
B10-2					
B11	0.4				D6@65
B12	0.8				D10@75
B10.3-1	0.0	2.11	388	9D25 2D16	
B10.3-2			372		
B13-1	0.0	2.07	398	10D32 2D13	
B13-2					
B14	0.0	2.04	398	14D32 4D13	
B17	0.4				D13@100
B15	0.0	1.99	402	18D35 2D13	
B16	0.0	2.05	394	18D41 2D13	
B18	0.4		397.5		D16@120

Size effect study

The results of experiments confirmed existence of size effect on shear strength of tested specimens. Test specimens cover a wide range of effective depth from 400mm to 1400mm. Variation of average shear stress taking into account concrete compressive

TABLE 2. GEOMETRIC AND MATERIAL PROPERTIES OF SPECIMENS

<table>
<tr><th rowspan="2">Beam</th><th rowspan="2">a/d</th><th colspan="7">Geometry size (mm)</th><th rowspan="2">f_c' MPa</th><th rowspan="2">P_u KN</th><th rowspan="2">P_{cr}^{sh} KN</th><th rowspan="2">δ_{peak} (mm)</th></tr>
<tr><th>L</th><th>c</th><th>a</th><th>d</th><th>h</th><th>b</th><th>b_s</th></tr>
<tr><td>B2</td><td rowspan="3">0.5</td><td rowspan="3">700</td><td rowspan="10">300</td><td rowspan="3">200</td><td rowspan="10">400</td><td rowspan="10">475</td><td rowspan="10">240</td><td rowspan="10">100</td><td rowspan="2">36.2</td><td>1550</td><td>525</td><td>3.16</td></tr>
<tr><td>B3</td><td>1536</td><td>625</td><td>4.78</td></tr>
<tr><td>B4</td><td>31.3</td><td>1951</td><td>700</td><td>1.85</td></tr>
<tr><td>B6</td><td rowspan="3">1.0</td><td rowspan="3">1100</td><td rowspan="3">400</td><td rowspan="2">31.3</td><td>1050</td><td>400</td><td>2.77</td></tr>
<tr><td>B7</td><td>1181</td><td>400</td><td>2.58</td></tr>
<tr><td>B8</td><td>37.8</td><td>1501</td><td>600</td><td>3.26</td></tr>
<tr><td>B10-1</td><td rowspan="13">1.5</td><td rowspan="4">1500</td><td rowspan="4">600</td><td>29.2</td><td>616</td><td>325</td><td>3.82</td></tr>
<tr><td>B10-2</td><td>23</td><td>703</td><td>278</td><td>5.28</td></tr>
<tr><td>B11</td><td>29.2</td><td>1025</td><td>350</td><td>15.96</td></tr>
<tr><td>B12</td><td>31.3</td><td>1161</td><td>300</td><td>7.05</td></tr>
<tr><td>B10.3-1</td><td rowspan="2">2250</td><td rowspan="2">450</td><td rowspan="2">900</td><td rowspan="2">600</td><td rowspan="2">675</td><td rowspan="2">360</td><td rowspan="2">150</td><td>37.8</td><td>1960</td><td>700</td><td>6.62</td></tr>
<tr><td>B10.3-2</td><td>31.15</td><td>1787</td><td>527</td><td>8.62</td></tr>
<tr><td>B13-1</td><td rowspan="2">3000</td><td rowspan="2">600</td><td rowspan="2">1200</td><td rowspan="2">800</td><td rowspan="2">905</td><td rowspan="2">480</td><td rowspan="2">200</td><td>31.63</td><td>2985</td><td>500</td><td>11.87</td></tr>
<tr><td>B13-2</td><td>24</td><td>2257</td><td>807</td><td>9.33</td></tr>
<tr><td>B14</td><td rowspan="2">3750</td><td rowspan="2">750</td><td rowspan="2">1500</td><td rowspan="2">1000</td><td rowspan="2">1105</td><td rowspan="2">600</td><td rowspan="2">250</td><td>31</td><td>3969</td><td>1100</td><td>9.27</td></tr>
<tr><td>B17</td><td>28.7</td><td>5214</td><td>1600</td><td>11.92</td></tr>
<tr><td>B15</td><td>4500</td><td>900</td><td>1800</td><td>1200</td><td>1305</td><td>720</td><td>300</td><td>27</td><td>5390</td><td>1500</td><td>11.91</td></tr>
<tr><td>B16</td><td rowspan="2">5250</td><td rowspan="2">1050</td><td rowspan="2">2100</td><td rowspan="2">1400</td><td rowspan="2">1505</td><td rowspan="2">840</td><td rowspan="2">350</td><td>27.3</td><td>5975</td><td>1900</td><td>10.57</td></tr>
<tr><td>B18</td><td>23.5</td><td>8396</td><td>2400</td><td>15.79</td></tr>
</table>

strength ($V_u / b.d.\sqrt[3]{f_c'}$) in terms of effective depth is shown in Fig.3. To eliminate a/d effect on ultimate shear stress of the beams, only a/d=1.5 is considered here. According to size effect investigation and theories it is evident that as the effective depth increases, the shear strength of the section decreases. The regression line is assumed to be a power function of effective depth *d*. The equation is round off and rewritten in the following form:

$$f(v_u) = \lambda(d^{-0.22}) \tag{1}$$

where in coefficient λ is a function of a/d ratio, reinforcement ratio and member's boundary condition. Since the three aforementioned parameters are constant for the beams used to produce Fig.3, $\lambda = 4.77$ is found to best fit to the experiment data points. In order to investigate practical aspects of size effect in design of structures, two Japanese design codes JSCE (Japan Society of Civil Engineers) and JRA (Japan Road Association) are

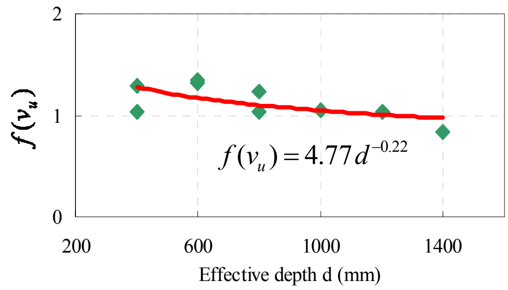

FIG.3 EFFECTIVE DEPTH VERSUS SHEAR FUNCTION $f(v_u) = V_u / bd\sqrt[3]{f'_c}$ FOR AV=0 AND A/D=1.5

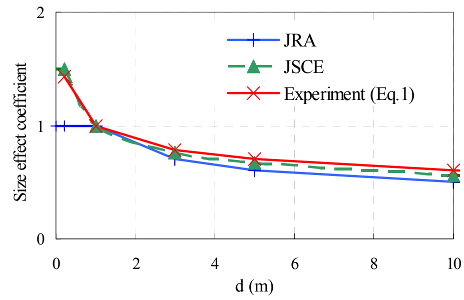

FIG.4 EFFECTIVE DEPTH VERSUS SIZE EFFECT COEFFICIENT

employed to be evaluated with test results. According to JSCE, shear stress varies in terms of $d^{\frac{1}{4}}$ while JRA proposed definition can be estimated by a function of $d^{\frac{1}{3}}$ to take into account size of specimen. Although the foregoing expression of Fig.3 is a crude approximation of size effect but it agrees well with that of proposed by JSCE code. There is, however, not a significant differences between JSCE and JRA size effect expression as can be seen in Fig. 4 and both expressions are attributed to a reasonable estimation of member depth effect. Size effect coefficient represents increase or decrease of shear strength in terms of effective depth. The maximum values for this coefficient set 1.0 and 1.5 by JRA and JSCE code respectively. In other words, in spite of JSCE code, which attributes 50% increase in shear strength capacity to size effect, JRA however does not allow any increase in shear strength for smaller effective depth. One reason for this might be the fact that JRA is usually dealing with structures with large components most of them larger than one-meter depth but JSCE should cover wider range of element size since it is to design various structures too. It is however noted that JRA accepts 40% higher shear strength for members with smaller depth ($d \leq 300\,mm$) where in linear design concept is applied (Part-IV, p.148).

Finite Element Simulation

The constitutive behavior of concrete is represented by a smeared crack model, which in the damaged material still continuum. Analytical scheme and finite element mesh discretization is shown in Fig.5. According to concrete crack model, two approaches can be highlighted as fixed crack and rotating crack theory. In the fixed crack model, once crack initiates in a finite element, the crack direction is calculated according to the principal stress direction. The crack direction is kept constant during further load increments and considered as the material axis of orthotropy. As a general case, principal stress directions need not to be coincide with axes of orthotropy and can rotate during loading process. This assumption produces a shear stress in crack surface. In order to prevent the effects of this artificially existed shear stress in the analysis, a shear retention factor as a reduction coefficient is always applied in this model. This factor can be either of a constant coefficient or varies during analysis as a function of crack width.

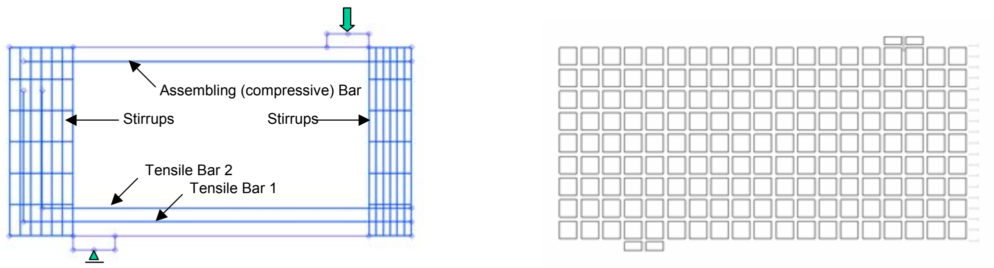

FIG.5. ANALYTICAL MODEL AND FE MESH DISCRETIZATION (SHRINK MESH)

Complication of this model manifests itself in definition of this parameter particularly when a constant value is assigned for entire analytical procedure.

Alternatively, rotating crack model is presented where the direction of the principal stress coincides to the direction of the principal strain. Since crack direction rotates according to the principal stress direction, no shear stress is generated on the crack surface and just two principal components need to be defined. In order to prevent consequent effect of shear retention factor definition in analysis, only the rotating crack approach is adopted in the present study as finial results. Specimens are partly modeled by FEM due to the symmetric geometry with 2D elements in plane-stress condition. Steel reinforcement is modeled as an elastic perfect plastic material with no hardening after the yield point.

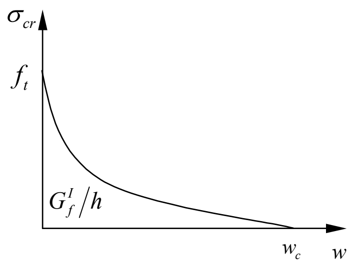

FIG.6. TENSILE CONCRETE MODEL

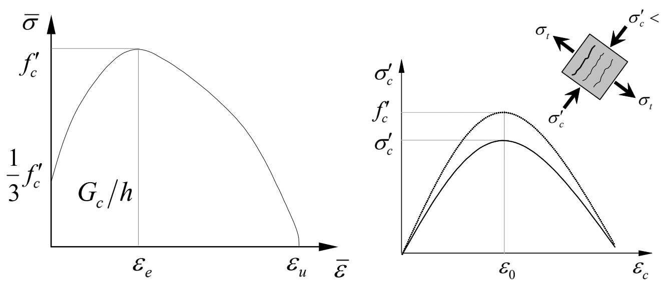

FIG.7. COMPRESSIVE CONCRETE MODEL AND SOFTENING DUE TO LATERAL TENSILE CRACKS

Concrete models

Concrete constitutive models are assumed in a fracture type material framework with constant released fracture energy during cracking process with a characteristic length parameter which is material property. This assumption eliminates mesh size effect accomplishes a mesh objective analysis.

Concrete in Tension

Concrete in tension is modeled by constitutive model suggested by Hordijk (1991) with a constant value of fracture energy shown in Fig.6. Concrete in tension before

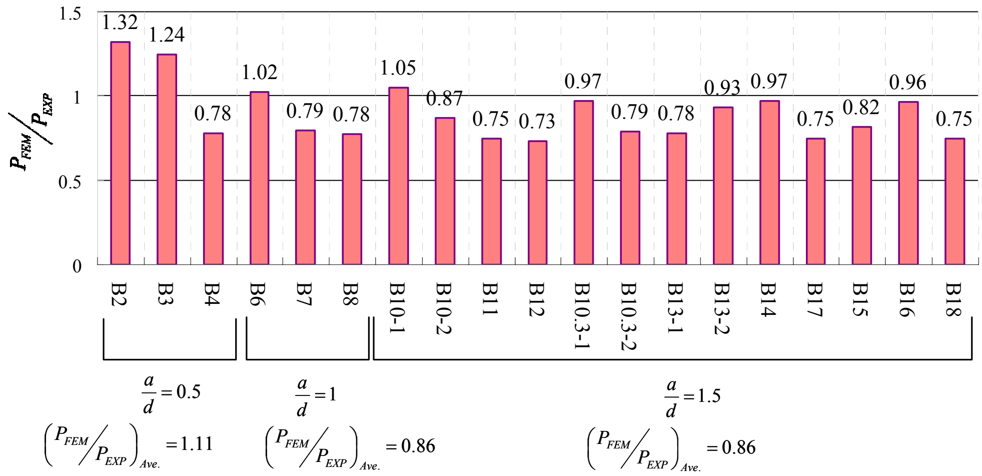

FIG.8. ANALYSIS VERSUS EXPERIMENT REPRESENTED BY P_{FEM}/P_{EXP} RATIO

cracking is assumed to be linear elastic. After cracking however, a softening branch forms and it is assumed that the descending path follows an exponential function of crack width derived experimentally and shown below

$$\frac{\sigma}{f_t}=\left\{1+\left(c_1\frac{w}{w_c}\right)^3\right\}\exp\left(-c_2\frac{w}{w_c}\right)-\frac{w}{w_c}\left(1+c_1^3\right)\exp\left(-c_2\right) \tag{2}$$

where w is the crack opening; w_c is the crack opening at the complete release of stress which is a function of fracture energy G_f defined by Equation 3; and σ is the normal stress in crack and f_t is the tensile strength of concrete in one dimension system or effective tensile strength in two dimension system. Values of the constants are, c_1=3, c_2=6.93.

$$w_c=5.14\frac{G_f}{f_t} \tag{3}$$

Tensile strength of concrete (for those specimens with no test results) and also tensile fracture energy G_f, Japan Society of Civil Engineers (JCSE, 2002) recommendations (Eq.4 and 5) are applied.

$$f_t=0.23f_c'^{\frac{2}{3}} \quad (MPa) \tag{4}$$

$$G_f=10(d_{\max})^{1/3}.f_c'^{1/3} \tag{5}$$

where d_{max} is maximum aggregate size in mm and G_F is fracture energy in N/m.

Concrete in Compression

Concrete in compression is supposed to follow a parabolic rout that has been modified (Feenstra, 1993) to take into account fracture energy of concrete (Fig.7). Following equations are representing this model, which in equivalent stress is determined in terms of equivalent strain.

$$\bar{\sigma} = \begin{cases} \dfrac{f_c'}{3}(1+4\dfrac{\bar{\varepsilon}}{\varepsilon_e}-2\dfrac{\bar{\varepsilon}^2}{\varepsilon_e^2}) & if \;\; \bar{\varepsilon} < \varepsilon_e \\ f_c'(1-(\dfrac{\bar{\varepsilon}-\varepsilon_e}{\varepsilon_u-\varepsilon_e})^2) & if \;\; \varepsilon_e \le \bar{\varepsilon} < \varepsilon_u \end{cases} \tag{6}$$

$$\varepsilon_e = \frac{4}{3}\frac{f_c'}{E_c} \tag{7}$$

Consequent to the length parameter association, ultimate strain will be a function of compressive fracture energy, length parameter *h*, f_c' and also ε_e as below

$$\varepsilon_u = 1.5\frac{G_c}{h f_c'} - \frac{11}{48}\varepsilon_e \tag{8}$$

Through this model concrete is assumed to be linear elastic up to $\frac{1}{3}f_c'$ therefore pre-peak energy will be taken into account by a correction factor $\frac{11}{48}\varepsilon_e$ in Eq.8. Furthermore, the concept of Modified Compression Field Theory (Vecchio *et al*, 1986) is associated in analyses by means of concrete compressive strength softening due to the lateral tensile cracks (Fig.7 right).

Load Capacity

Figure 8 shows ultimate loads predicted by analysis over test results ratios. The results show acceptable as well as consistent numerical prediction for beams with a/d > 0.5, which in most of the predictions fall below load capacities obtained by experiment. In contrast, for a/d=0.5, at least two specimens B2 and B3, analyses have predicted higher load capacity with extremely lower displacement than the experiment. It is expected, however, that for beams with very low a/d ratio, sliding bond model as well as employing an interface element between supporting plate and concrete body will correct analytical response to a certain level. The latter will eliminate undesired steel plate stiffness contribution to the entire structure stiffness matrix and also eliminates stress concentration in adjacent elements. Averaged ratio for a/d=0.5 is 1.11 and for a/d>0.5 is 0.86 (Fig.8). The results for at least a/d>0.5 shows very acceptable prediction with about 15% safety margin.

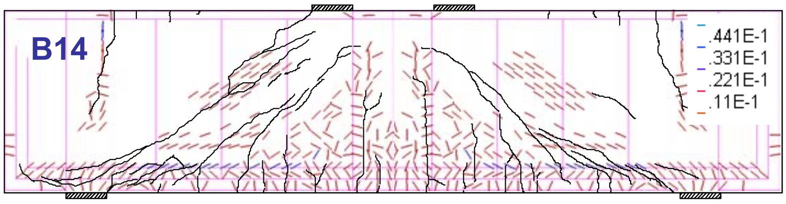

FIG.9. B14 CRACK PATTERNS OF ANALYSIS AT ULTIMATE STATE VERSUS EXPERIMENT

Experiment showed that shear crack initiated at about 40% of the ultimate load and full shear crack will be formed approximately in $0.5P_u$ but still beam sustained load capacity to about 80-90% of the ultimate load. Afterward shear cracks were severely widened and extended to compressive zone. Shear sliding of concrete pieces around shear crack could be clearly observed with bare eyes. This point is considered the ultimate capacity of beam in shear by a number of design codes, which the beam is in serious irreversible circumstances. According to this definition if numerical analysis is aiming to produce results for practical application such as RC member design, in average having $P_{Analysis} \approx 0.80\, P_{Exp.}$ can be considered as a quite satisfactory result.

Crack Patterns

Crack patterns depicted in Fig.9 shows very accurate prediction by analysis where in almost all important cracks are captured. In the rest of the specimens also predicted cracks were in good agreement with experiment. This implies that adopted finite element analysis of this study can be adequately applied for damage evaluation of underground structures under seismic loads. Analytical crack patterns are drawn in shadow of experimental cracks (black lines) for better evaluation. It is noted however that in analysis all cracks are shown in figures without any filter where crack width is presented in five colored levels.

Wall-type piers under cyclic load

It is well explained by quite number of experimental investigations that for members with small shear span to depth ratio, conventional shear resistance mechanism yields very conservative prediction. Experiment results of this study also confirmed formation of shear resistance mechanism similar to that observed in deep beams. Two RC walls have been tested in Public Works Research Institute during the year 2004 in order to investigate shear behavior of such members under cyclic

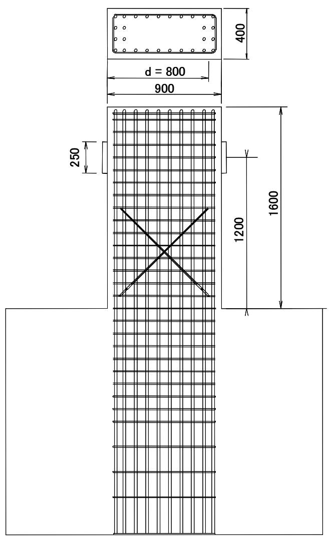

FIG.10. DETAIL OF SPECIMENS

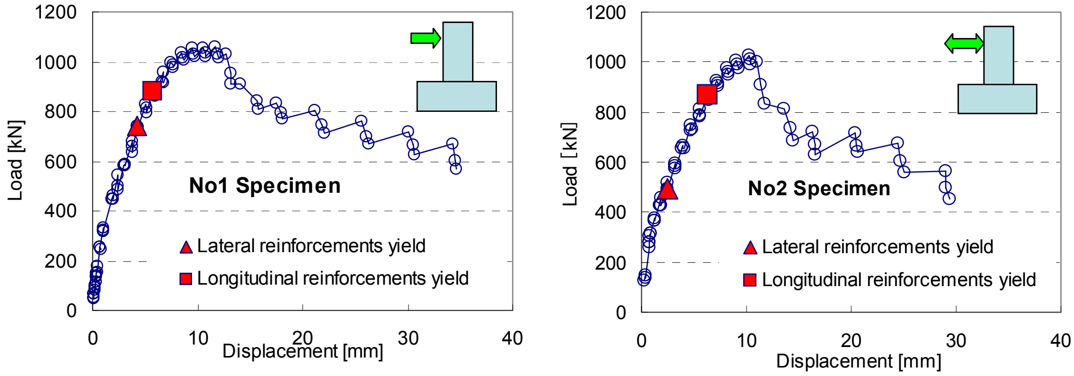

FIG.11. ENVELOPE OF CYCLIC RESPONSE OF SPECIMENS

load condition. Existence and development of diagonal cracks have been measured by two displacement transducers installed in locations with highest possibilities of shear cracks occurrence.

Test specimens comprise of two RC walls with shear span to depth ratio of 1.5 under one and two directional cyclic loads. Longitudinal and lateral rebar are smeared out all over the wall in order to produce a smooth distribution of stress over the member. Structural detail of specimens is shown in Fig.10 and Fig.11 illustrates envelope of cyclic responses of both specimens in positive direction. It is observed that in one-directional loading condition (No.1), shear reinforcement yielded in higher level of load than wall No.2. In contrary, longitudinal reinforcements who represent bending capacity of the member yielded in almost identical load level. This implies that shear capacity of the member is more sensitive to loading pattern than that of bending.

Analytical predictions in two cases of monotonic and cyclic (envelope is shown here) are compared with test results in Fig.12 for wall No.2. The results are in good agreement with experiment. Deterioration of load capacity in cyclic load is clearly seen in this figure where in peak load is slightly smaller in comparison with monotonic load condition. As for post-peak regime, cyclic load response experiences a sudden decrease just a few cycles after the peak which is also attributed to progressive deterioration of bond between steel and concrete.

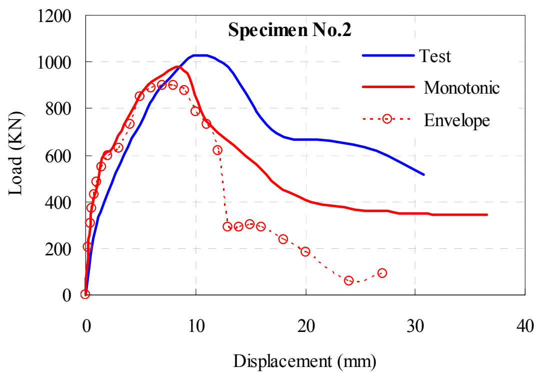

FIG.12. NO.2 SPECIMEN RESULTS

Conclusion

Investigation on RC deep beams behavior and their modeling with nonlinear finite element analysis is presented in this paper. The material model proposed by Hordijk and Feenstra are applied for concrete in tension and compression respectively in fracture mechanics framework to eliminate mesh dependency of the results. The applied methods with the rotating crack model, however, could predict RC deep beams response to monotonic static load with acceptable accuracy. In most of the specimens predicted peak loads have been lower than their relative test results. This ensures a safety margin for design of RC members if load capacity of the member is the major concern of design. Predicted crack patterns are also evaluated by experiment observation. The main findings of this paper are drawn as follows:

1. Pre-peak regime could be properly captured by the applied material models and finite element analysis.
2. Correlation between predicted cracks by analysis and monitored during test process is suitably adjusted. Almost all important cracks including those of tensile cracks on upper face of the beam near to the end region are very well predicted. The predicted crack patterns therefore can be well utilized for damage evaluation of RC members.
3. The method can be applied for larger number of RC elements in the form of parametric study to avoid time consuming and costly experimental works.
4. Acceptable results have also been obtained by applying the presented finite element method in prediction of RC wall-type pier behavior with shear failure potential.

References

Feenstra, P.H., "*Computation aspects of biaxial stress in plain and reinforced concrete",* PhD thesis, Delft University of Technology, 1993.

Hordijk, D.A., *Local approach to fatigue of concrete,* PhD thesis, Delft University of Technology, 1991.

Japan Society of Civil Engineers, "*Standard specifications for concrete structures"*, Structural performance verification (in Japanese), Tokyo, March, 2002, pages 67 and 190.

Kwak, H., and Flippou F.C., *Finite element analysis of reinforced concrete structures under monotonic loads*, Report No. UCB/SEMM-90/14, Department of Civil Engineering, University of California Berkeley, Nov. 1990, pp.32-35.

Salamy, M.R., Kobayashi, H., Unjoh, Sh., Kosa, K. and Nishioka, T., "*A code-based comparative study on RC deep beams behavior with shear span to depth ratio between 0.5 and 1.5"*, 8th Symposium on Ductility Design Method for Bridges, Tokyo, Feb. 1-2, 2005 pp. 293-298.

Vecchio, F. and Collins, M.P., *The modified compression field theory for reinforced concrete elements subjected to shear*, ACI structural journal, V.3, No.4, 1986, pp. 219-2